



Trinity College Dublin
Coláiste na Tríonóide, Baile Átha Cliath
[The University of Dublin](#)

School of Physics

Computer Simulations of Three Dimensional Foams

Aleksander Alan Prymek

April 8, 2023

A dissertation submitted in partial fulfilment
of the requirements for the degree of
Theoretical Physics

Declaration

I hereby declare that this dissertation is entirely my own work and that it has not been submitted as an exercise for a degree at this or any other university.

I have read and I understand the plagiarism provisions in the General Regulations of the University Calendar for the current year, found at <http://www.tcd.ie/calendar>.

I have also completed the Online Tutorial on avoiding plagiarism 'Ready Steady Write', located at <http://tcd-ie.libguides.com/plagiarism/ready-steady-write>.

Signed: _____

Date: _____

Abstract

Most computer simulations in the area of foams have been performed in the dry limit, that is, on foams where the liquid fraction is extremely small, usually less than 1%. Wet foams (liquid fraction > 20%), on the other hand, do not receive as much attention; nonetheless, their significance cannot be overstated. In this project, wet foams in three dimensions are simulated using the Morse-Witten model as well as the more approximate Durian model. The software was developed to equilibrate foam structures in confinement. High-quality, realistic images of deformed bubbles described by the Morse-Witten theory were then realised using the 3D graphics software Blender in order to better understand the nature of the bubble-bubble interaction.

Contents

1	Introduction	1
1.1	Soft Matter	1
1.2	Foam	2
1.3	Dry and Wet Foams	3
1.4	Computer Simulations	4
2	Background and Theory	5
2.1	Durian Model	5
2.2	Morse-Witten Model	6
2.2.1	Single Contact	7
2.2.2	Multiple Contacts	8
3	Project	10
3.1	Foam Simulation	10
3.1.1	The ‘Cage’ Problem	10
3.1.2	Finding Equilibrium	11
3.2	Foam Visualisation	12
4	Evaluation	13
4.1	Equilibration	13
4.2	Energy Calculation for Two-Bubble System	15
4.2.1	Durian Model	15
4.2.2	Morse-Witten Model	16
4.3	Foam Visualisation	17
5	Conclusion	18
A1	Appendix	22

List of Figures

1.1	Foam buoyed on water. Bubbles in foams are not spherical - their shape depends on the liquid fraction ϕ (the volume fraction of the liquid phase). In the top layers, most of the liquid has drained, resulting in large contact areas between bubbles. In the bottom layer, the liquid fraction is large enough to allow bubbles to attain a close-to-spherical shape. Source: [1]	1
1.2	A slice of the universe showing galaxy clusters arranged in a foam-like structure. Source: [2].	2
1.3	Photograph showing at least five layers of bubbles ($R = 0.25\text{mm}$) arranged in an FCC packing. Source: [3]	4
2.1	In the Durian model, bubbles are treated as non-deformable spheres. The force relation is usually taken to be a Hooke's law: $F = -k_D\delta$, and often the proportionality constant is set to $k_D = \frac{\gamma}{2}$, where γ is the surface tension. The distortion x is always negative and is equal to $-\gamma/2$	6
2.2	a. An exaggerated reaction of a bubble to a point force. Source: [4]. b. A bubble buoyed against a flat wall. The blue outline is the shape defined by eq. (4) with the singularity capped. The black dotted outline shows a sphere with a coinciding centre of mass and of the same volume as the bubble. The critical angle θ_c as well as the perturbed radius $R(\theta) = R_0 + x$ are indicated.	7
3.1	Face-centred cubic bubble structure. In red is the central free-to-move bubble; in grey are the artificially-fixed bubbles, i.e., the cage bubbles.	11
4.1	FCC structure equilibration using Morse-Witten model and fixed cage constraint (liquid fraction= 0.2). The top left image shows the initial structure, while the top right shows the final, equilibrated structure. As expected from the symmetry, the central bubble was pushed to the origin. The bottom graph shows the magnitude of the net force acting on the central bubble at each step of the process.	13
4.2	FCC structure equilibration using Morse-Witten model and harmonic potential constraint (potential width= 1.9). The top left image shows the initial structure, while the top right shows the final, equilibrated structure. As expected from the symmetry, the central bubble was pushed to the origin. The bottom graph shows the magnitude of the net force acting on the central bubble at each step of the process.	14

4.3 Left: Numerical and analytical overlap energy of a two-bubble system as a function of the potential width obtained using the Durian model. Right: Numerical and analytical solution for the equilibrium position of the bubbles in the two-bubble system as a function of the potential width.	16
A1.1 A cross-section of a bubble in equilibrium buoyed against a flat wall exerting a vertical point force.	22
A1.2 Two bubbles pressing against each other with contact force of $f = 2$	22
A1.3 Top: A single FCC bubble with and without singularities capped. Bottom: A single FCC cell with and without singularities capped.	23
A1.4 Towers of vertically stacked bubbles under gravity.	23

1 Introduction

The main objective of this work is the development of simulations of three-dimensional wet foams. To do so requires the design and use of software capable of generating a foam system and progressing it in time towards an equilibrium. This is the first major milestone of this project. The second is the creation of a script, which, given data generated by the main software, produces a 3D graphical visualisation of the computed structures.

The study of foam physics is a relatively small area of soft (condensed) matter physics, which itself is a sub-field of an even larger field of condensed matter physics. The term soft matter encompasses a large variety of materials: colloids, emulsions, polymers, granular materials, and - of course - foams.

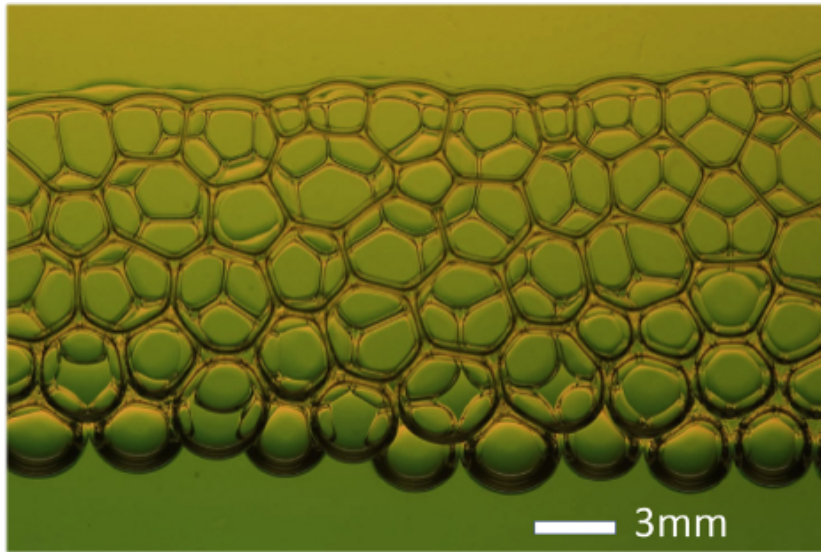


Figure 1.1: Foam buoyed on water. Bubbles in foams are not spherical - their shape depends on the liquid fraction ϕ (the volume fraction of the liquid phase). In the top layers, most of the liquid has drained, resulting in large contact areas between bubbles. In the bottom layer, the liquid fraction is large enough to allow bubbles to attain a close-to-spherical shape. Source: [1]

1.1 Soft Matter

Although the project is entirely centred on simulations of foams, we should first take, for a brief moment, a broader view of the field of soft matter to better understand the problem at hand. Since such a huge diversity of materials is contained in the ambit of soft matter, there

must be something fundamentally similar about these materials. They are obviously, as the name suggests, soft, or in other words, easily deformable - but what makes them such?

The answer to the softness of soft matter lies in the presence of mesoscopic scale particle-like entities (or, for convenience, simply particles). Foams, for example, are composed of bubbles; colloids are aggregates of colloidal particles. In any case, particles that are much smaller than the bulk material but much larger than an individual atom make up the material. The key consequence of this property is that the interactions between the mesoscopic particles - and not the interactions between individual atoms - define the elastic response of the material as a whole; and due to their large size, the elastic moduli must be necessarily small; i.e., the material must be soft [5].

Although some soft materials do experience thermal fluctuations (as will be mentioned later), they do have a tendency to self-assembly and evolve towards equilibrium. The exact structure of soft material is determined by energy (or, equivalently, surface area) minimisation.

1.2 Foam

For a long time, foams and foam-like structures have been of great practical importance as they are ubiquitous in nature on all of its scales: from quantum level (e.g. quantum foams, quantum dots [6]) through human scale (e.g. fire extinguishers, beer froth) to the scale of the entire universe (e.g. distribution of galaxy clusters [2]).

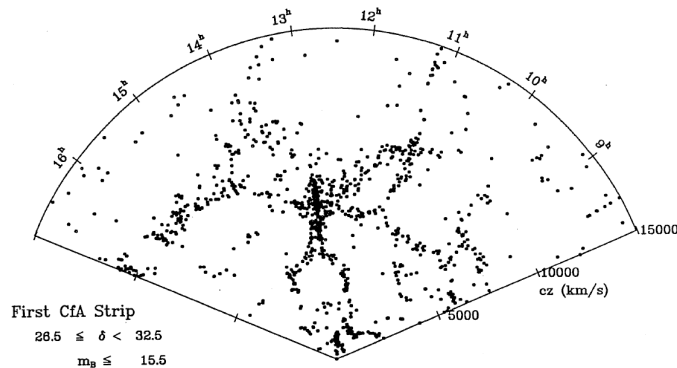


Figure 1.2: A slice of the universe showing galaxy clusters arranged in a foam-like structure. Source: [2].

Before we delve any further it is important to answer the following question: what exactly is foam?

A foam is a structured fluid in which gas bubbles are separated by thin liquid films and the volume fraction of the continuous liquid phase (liquid fraction) is small [7]. The liquid fraction determines many characteristics of foam, most importantly the shape of the bubbles, and defines two limits: dry (liquid fraction $\sim 1\%$ or less) and wet (liquid fraction $> 20\%$) [8].

Foams share many physical properties, such as aging and structure, with emulsions; but, they differ from colloids in a significant way. The energy of an N -bubble foam is $E = \gamma \sum_i^N S_i$, where S_i is the surface area of the i th bubble, and γ is the surface tension. For a typical bubble

($R \approx 100 \mu\text{m}$ and $\gamma \approx 0.03 \text{ N m}^{-1}$), the energy is of the order of 10^{-8} J , which renders the thermal energy, $kT \sim 10^{-21} \text{ J}$, irrelevant [9]. The same cannot be said about colloids which should be thought of as being in a constant state of random motion as they do experience fluctuations due to the Brownian motion since colloidal particles can be much smaller than the usual air bubble [10].

1.3 Dry and Wet Foams

As liquid fraction decreases bubbles get closer to each other. When the value reaches the critical liquid fraction, given by $\phi_c = 1 - \frac{\pi}{3\sqrt{2}} \approx 0.26$, bubbles come into contact and thus deform. Their surface area increases as a facet at their contact is created. A larger surface area results in higher energy, and so, a repulsive interaction force arises. Clearly, the (local) liquid fraction has huge importance in the physical properties of the foam.

In the dry limit, most of the liquid is expelled and bubbles are heavily distorted from their original spherical shape even in monodisperse foams (see the top bubble layers in fig. 1.1). They are closely packed and form large contact areas with their neighbours to a point where they attain shapes similar to that of a polyhedron. Most of the research in the area of foams has been performed in this limit partially due to the development of computational software called Brakke's Surface Evolver that allows for simulations of foam structures for which the total surface area is minimal [11]. The software works best in the dry limit, and, even though it is capable of handling any liquid fraction, it runs into problems when simulating wet foams. The software depends on surface triangulation - it divides surfaces into triangles (it is common practice in computer graphics) in order to create a finite number of faces to imitate the spherical/curved surfaces in foam. As contact areas become smaller, i.e., as we move deeper into the wet foam regime, bubbles become rounder while the contact areas become smaller. To effectively represent such structures, the Surface Evolver needs to divide bubbles' surfaces into an increasingly large number of triangles. But, the larger the number of elements of which the system comprises, the more computationally expensive the simulation becomes. In the wet limit, the cost is too high, resulting in simulations no longer being feasible.

In the wet limit, bubbles remain mostly spherical as contact forces are minimal (see the bottom row of bubbles in fig. 1.1). In many ways, considerations on wet foams are closely related to those of weakly compressed emulsions [12, 13]. The progress in this limit was more theoretical in nature, since, as implied above, there is a lack of stable and reliable software capable of simulating wet foams. (This project aims to fill this gap and allow for better numerical simulations in this limit.) Additionally, analytical descriptions were made easier thanks to the natural symmetries occurring in wet foams. Crystal-like bubble structures have been achieved experimentally (in two dimensions) as early as 1947 by Bragg and Nye [14], but also recently by A. van der Net et al. [3]. Interestingly, these macroscopic systems order spontaneously and realise FCC- and HCP-like structures. This is surprising, as systems composed of similar-sized particles do not conform to any comparable symmetry. The exact reason behind this phenomenon is still a mystery; although, according to Net et al. "[t]he answer may lie in the particular form of the bubble–bubble interaction and the relation of its magnitude to that of gravity in this size range".

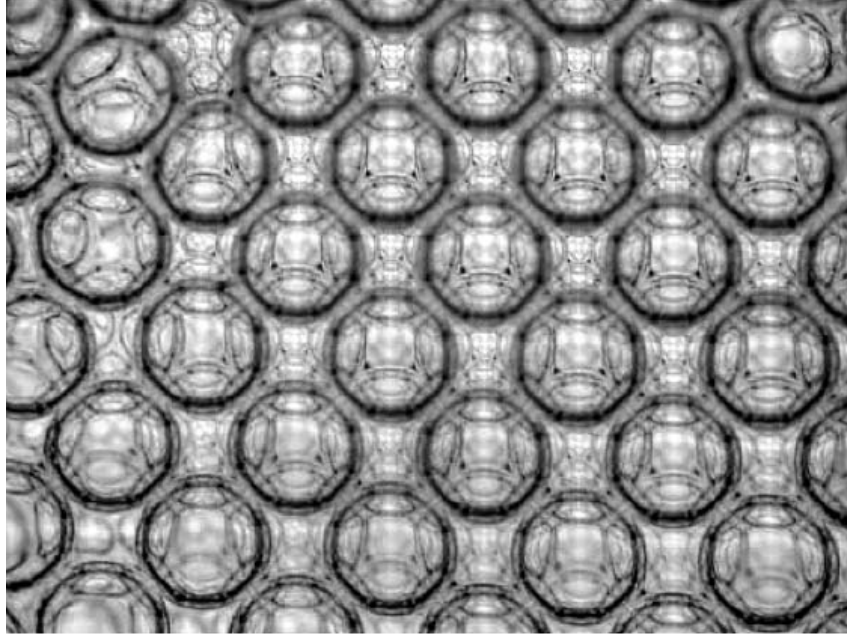


Figure 1.3: Photograph showing at least five layers of bubbles ($R = 0.25\text{mm}$) arranged in an FCC packing. Source: [3]

1.4 Computer Simulations

When it comes to the numerical simulations of wet foams, the main problem is the complicated shape of bubbles [15]. The shape of a bubble must satisfy two conditions: the free bubble surface must have a constant mean curvature, and it must meet the film at zero contact angle [13]. A theory that satisfies said requirements is that of Morse and Witten. It was derived from the Young-Laplace law which relates the pressure difference to the shape of a bubble/droplet (hence, it satisfies the first condition stated above). The theory can be said to be exact in the asymptotic wet limit (i.e. when liquid fraction approaches the critical liquid fraction, ϕ_c), and to be non-local, as bubbles are represented by points placed at their centroids with central forces acting on them (hence, it satisfies the second condition), where each force depends on all the other local contact forces of the bubble.

The development of what we now call the Morse-Witten model was pivotal in wet foam research and is extensively used in what follows.

2 Background and Theory

To this day, the exact description of the repulsive force due to contact between two bubbles remains a conundrum. In the majority of simulations, an easy route was taken by assuming that the force is pairwise additive; while it is a reasonable approximation, lamentably for many researchers, it is unfounded and leads to incorrect analytical results [16]. A more fundamental approach is that of Morse and Witten: In their work on elasticity of weakly compressed droplets [12] - a principal work in the area of wet foams - they derived an expression for this type of interaction accurate in the wet limit where all forces are nearly null. Their description included a logarithmic term granting a very unique behaviour to bubbles and foams.

In this project, we focus entirely on wet monodisperse foams. Below, packings of bubbles without static friction are considered, and in all equations, as well as simulations, dimensionless units were used by normalising forces, energies, pressure, and lengths by γR_0 , γR_0^2 , $\frac{\gamma}{R_0}$ and R_0 , respectively; with γ being the surface tension and R_0 being the unperturbed bubble radius.

2.1 Durian Model

The difficult part of the numerical foam simulations is the treatment of bubble shape and the bubble-bubble interactions. The simplest formalism of these interactions is that of central pairwise forces first introduced to foam simulations by Durian [17]. Most commonly, for this type of interaction, a harmonic elastic force proportional to the overlap of the bubbles is used while bubbles are represented as perfect spheres that do not deform but overlap (see fig. 2.1). Of course, this is not in tune with nature, where, when two bubbles are brought in contact, they adjust their shape, rather than interpenetrate, and expand laterally almost as if they were incompressible. Incompressibility, in fact, is a good approximation in a majority of cases apart from some industrial processes since, in most simulations, Laplace pressure is an order of magnitude smaller than the bulk compression modulus of the internal fluid [12, 18].

In the Durian model, two bubbles are said to be in contact if the distance between their centres is smaller than the sum of their radii. The coordinates of a contact point are then defined to be halfway on the line joining the centroids. This pleasant simplicity is due to the rigidity of bubbles and allows the model to be used efficiently for vast foam structures, alas, with poor accuracy. Note that, in this model, bubbles are fully defined by the centre of mass and radius alone.

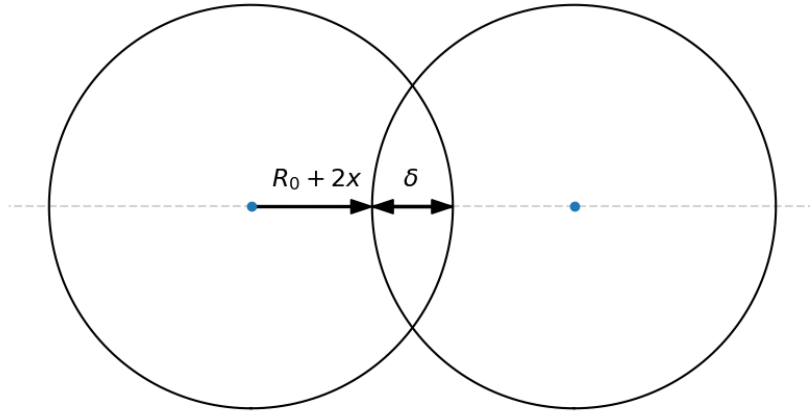


Figure 2.1: In the Durian model, bubbles are treated as non-deformable spheres. The force relation is usually taken to be a Hooke's law: $F = -k_D\delta$, and often the proportionality constant is set to $k_D = \frac{\gamma}{2}$, where γ is the surface tension. The distortion x is always negative and is equal to $-\gamma/2$

Usually, when using the Durian model, the magnitude of the contact force is defined using Hooke's law, namely,

$$f = -k_D\delta, \quad (1)$$

where δ denotes the overlap between two bubbles. Assuming that the bubbles are in contact and that they are a distance r away from the origin, we can define the overlap as

$$\delta = 2(R_0 - r), \quad (2)$$

where R_0 is the radius of a bubble (after normalisation it's unity).

While, in the wet limit, the bubbles experience very limited force and are little deformed, they are deformed nevertheless, and this deformation may be of interest. Reducing the geometry of the bubble to a perfect sphere will not allow for investigation of the way individual bubble reacts to forces from contacting neighbours and prevents us from accounting for the non-local effects of a contact force. Another drawback of this formalism is that harmonic force does not produce qualitatively adequate results, and hence, leads to incorrect analytic predictions of the bubble's and foam's elastic mechanical response.

2.2 Morse-Witten Model

A much more elaborate formalism was developed by Morse and Witten [12]. The derivation behind this approach is fairly complicated and lengthy, hence, the proof will not be replicated in full in this manuscript (explanation and simplification can be found in [1]). The bubble-bubble interaction in this approach is rigorously derived from the Young-Laplace law, which relates the shape of a soft particle, or more specifically its local curvature C , to the difference in its internal and external pressures, $\Delta p \equiv p_{\text{internal}} - p_{\text{external}}$. Denoting the surface tension as γ , we can write the Young-Laplace law as:

$$\gamma C = \Delta p. \quad (3)$$

The above equation, when expanded using spherical harmonics, yields a formula for the equilibrium profile of a single bubble,

$$R(\theta) = R_0 + \delta R(\theta) = 1 - fG(\theta), \quad (4)$$

where

$$G(\theta) = -\frac{1}{4\pi} \left\{ \frac{1}{2} + \frac{4}{3} \cos(\theta) + \cos(\theta) \ln \left[\sin^2 \left(\frac{\theta}{2} \right) \right] \right\}, \quad (5)$$

which is only dependent on the angle θ , that is, the angle between a point on the particle's surface and a contact point subtended at the bubble's centre of mass.

Furthermore, assuming forces much smaller than a unity, Morse and Witten found that the deformation energy due to contact between two particles scales as $E \propto f^2 \ln(\frac{1}{f})$. If we compare this to the standard Hooke's law used in the Durian model we get a logarithmically soft effective spring constant. From this, we obtain an unprecedented force law, where $x \propto f \ln(f)$, which warrants a status of a canonical force of nature similar to those of Hooke or Hertz [1].

2.2.1 Single Contact

When eq. (4) is plotted (see fig. 2.2a), it is clear that it describes a bubble's response to a point force with $\delta R(\theta)$ being the radial displacement of each point on the bubble's surface.

Let's consider a bubble immersed in a liquid being buoyed against a flat wall as is schematically shown in fig. 2.2b. The circular contact area is covered by a thin wetting film which we treat as infinitesimally thin. To analyse the shape of the bubble we only consider the case where the contact angle is zero and reduce the force due to the wall acting on the bubble to that of a point force (since we assume in the wet limit contact areas are substantially smaller than the surface area of a bubble), so as to allow us to use the equations defined above.

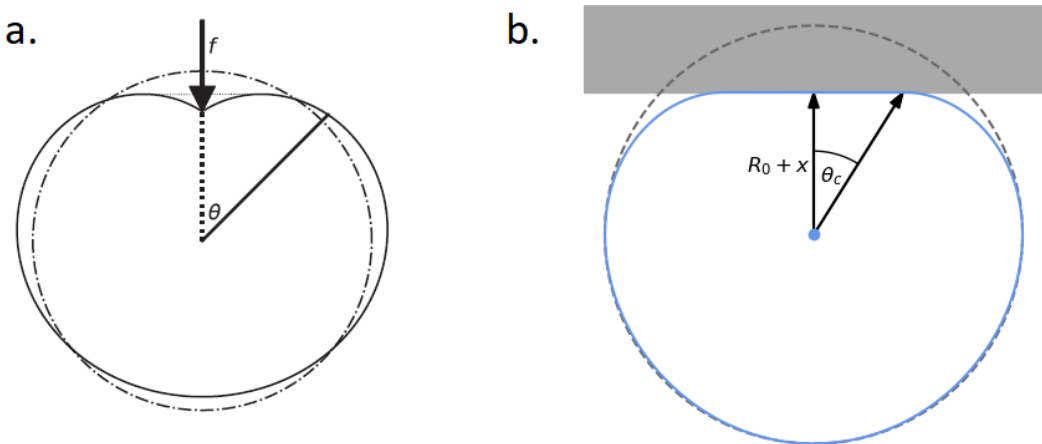


Figure 2.2: a. An exaggerated reaction of a bubble to a point force. Source: [4]. b. A bubble buoyed against a flat wall. The blue outline is the shape defined by eq. (4) with the singularity capped. The black dotted outline shows a sphere with a coinciding centre of mass and of the same volume as the bubble. The critical angle θ_c as well as the perturbed radius $R(\theta) = R_0 + x$ are indicated.

As the bubble comes into contact with the wall, the contact force squishes the bubble longitudinally. In order for the bubble to preserve its volume, it must bulge laterally. Note that $G(\theta) \rightarrow \infty$ as $\theta \rightarrow 0$, i.e., a singularity exists at the point of contact; this is of course an unwanted behaviour for a bubble pressing against a wall (or against another bubble). For a more proper description of a bubble's shape, eq. (4) is only used for $\theta > \theta_c$, where θ_c is the critical angle - for a single contact, it is the azimuthal angle created by the outermost point on the circular flat facet (see fig. 2.2), and to a leading order $\theta_c = \sqrt{\frac{f}{2\pi}}$, which is found by noting that the bubble interface must be horizontal at $\theta = \theta_c$. For $\theta < \theta_c$, there is no one way of dealing with the problem: if only one contact force is acting on a bubble, especially if it is due to a wall or a bubble of equal volume, we can assume the facet to be perfectly flat and simplify the problem to that of finding a tangent plane; however, for bubbles with multiple neighbours, such as those in FCC or HCP structures (both with a coordination number of 12), finding an accurate way of capping the singularities becomes more challenging as the contact area is no longer flat. (On how the problem was approached and solved see Section 3.2.)

2.2.2 Multiple Contacts

Theory regarding multiple contacts of a single bubble was the main objective of Morse and Witten [12] and naturally, it is essential for simulations of entire foams, or, for example, a single bubble confined by several walls. An analytical law for bubbles with multiple contacts was first derived by Buzzo and Cates [13] and later expanded by Höller and Cohen-Addad [16]. Hereunder contacts for each bubble are labelled by an index i and the modulus of the associated force is labelled by f_i .

The profile of a bubble with multiple forces acting on it is found by simply summing up $\delta R_i(\theta)$ present in eq. (4). That is,

$$R(\theta) = R_0 + \sum_i \delta R_i(\theta) = 1 - \sum_i f_i G(\theta_i). \quad (6)$$

When simulating dynamics of foam, the essential properties to be calculated are forces due to each contact, $f_i(x_i)$. The Morse-Witten theory, however, gives us the inverse relation which is also dependent on all the other forces:

$$x_i = \frac{1}{24\pi} \left[5 + 6 \ln \left(\frac{f_i}{8\pi} \right) \right] f_i - \sum_{j \neq i} G(\theta_{ij}) f_j. \quad (7)$$

Since this many-body interaction equation is non-linear, it cannot be easily inverted; hence, a special algorithm described in [16] is used to solve it numerically. The steps of the algorithm are as follows:

- (a) Given a bubble, for each contact point, calculate the overlap δ_i , and then the distortions x_i . δ_i can be easily found as positions and radii of all bubbles are known.
- (b) Estimate the contact forces using Hooke's law: $f_i(x_i) = -k_D x_i$.
- (c) Insert the estimates into the logarithmic term of eq. (7).
- (d) Solve resulting linearised equation using matrix inversion to obtain a new set of force estimates.

- (e) Check whether the forces converged to a solution.
 - (a) If not, return to the step (c) with the new estimates.
 - (b) Otherwise, end the algorithm.

The above algorithm is used for each bubble separately.

Unfortunately, bubble's deformations result in many problems in the correct implementation of the model. As mentioned previously, bubbles are treated as incompressible, and so, when one is brought in contact with another bubble (or a wall) they adapt their shape by squishing longitudinally and bulging laterally (see fig. 2.2a). This change in shape, in turn, may bring the bubble in contact with nearby bubbles, or alternatively, the bubble may lose contact with a neighbour. Due to this behaviour, it is extremely challenging to calculate and track contact points, especially as the contact point must not necessarily be on the centre-to-centre line. This would be a serious obstacle for numerical simulation of foams using the Morse-Witten model, if not the fact that, in the wet limit, the deformations are minimal, and so, they can be ignored without significant loss in accuracy.

3 Project

3.1 Foam Simulation

3.1.1 The ‘Cage’ Problem

Foams consist of hundreds, if not thousands, of bubbles. Any attempt to simulate such a huge system would be extremely expensive computationally - often to the point of not being feasible. For this reason, it is of interest to create a system containing fewer bubbles bounded by some constraints that would allow preserving the bulk properties of the foam. Hence, we define the ‘cage’ problem, where several bubbles are isolated from the environment using a ‘cage’.

In this project, two types of cages were considered. First - the crudest and the most faithful to its name - way of constructing the cage is by fixing artificially in place the outer bubbles, effectively confining the system to a fixed volume. For example, consider an FCC cell: it has 13 bubbles in total - 12 outer and 1 internal (see fig. 3.1). The 12 outer bubbles would then be immobilised, creating a fixed cage around the central free-to-move bubble. This approach is not ideal: it creates two classes of bubbles - fixed and moveable - which is unnatural and makes the expansion of the system arduous as the fixed bubbles need to be identified manually. On the bright side, it only requires tracking and updating the position of the moveable bubbles. Overall, it is the faster, but less accurate approach.

The second way of creating a cage is by placing all bubbles in a slightly modified harmonic potential such that it is zero within a certain distance from the origin. Mathematically, it can be written as:

$$V(r; r_0) = \begin{cases} k_p(r - r_0)^2, & r > r_0 \\ 0, & r \leq r_0 \end{cases}, \quad (8)$$

where k_p is a constant, r is the distance of a bubble’s centre of mass from the origin, and r_0 is half of the total ‘width’ of the potential. In this strategy, all bubbles are treated in the same manner, rendering the system more in tune with nature. Not surprisingly, it levies higher computational cost as contact points of all bubbles need to be tracked, rather than just those of the moveable bubbles.

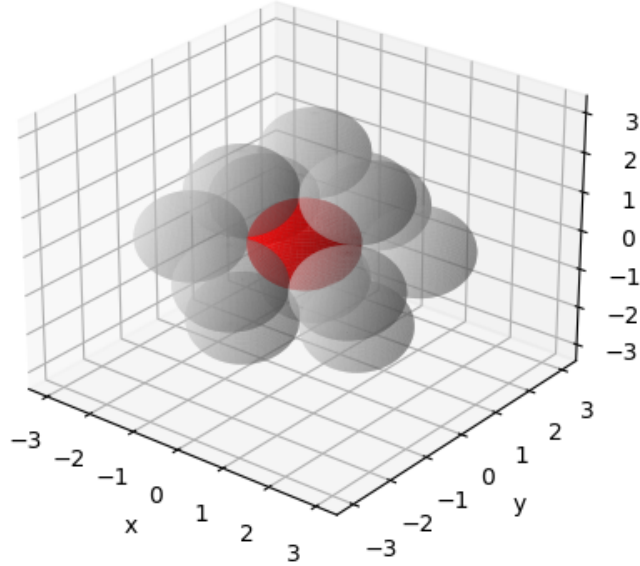


Figure 3.1: Face-centred cubic bubble structure. In red is the central free-to-move bubble; in grey are the artificially-fixed bubbles, i.e., the cage bubbles.

3.1.2 Finding Equilibrium

Given a system and its constraints, to simulate a set of interacting bubbles, we need to propagate the system in time until it reaches an equilibrium state. To do so we must calculate the forces acting on all bubbles and appropriately update their positions. For this task, the algorithm presented in [4], originally used for a 2D system, was adapted to 3D bubbles. The modified version contains the following steps:

- (a) Define the system (centre positions and radii of all bubbles).
- (b) Calculate and store the coordinates of all contact points.
- (c) For each bubble:
 - (i) calculate force exerted by each contact point;
 - (ii) calculate and store the net force.
- (d) Translate each bubble by a distance proportional to, and in the direction of, the net force acting on it.
- (e) Re-calculate contact points.
- (f) Check whether the net force acting on each bubble vanished.
 - (i) If the net forces have not vanished, return to the step (c).
 - (ii) Otherwise, the system is equilibrated, and the simulation can be ended.

Initially, bubbles were translated asynchronously; that is, a net force on a bubble was calculated, said bubble was then translated, and before moving to the calculation of the net force on the next bubble in the sequence, contacts were updated. It was found that this order of updates results in larger than expected distortions in the final, equilibrated structure compared to the initial one. This is because, if a bubble was translated partially in a non-radial direction,

in symmetric structures such as FCC or HCP, it would result in a ripple-like effect and cause rotatory displacement to (almost) all other bubbles. Hence, instead, net forces on all bubbles are calculated first, and bubbles are translated simultaneously.

To prevent occurrences of undesirable situations where a bubble moves too far in a single step and comes exceedingly close to a neighbour or, worse, passes through it, the maximum translation is capped by a value of one-tenth of the default bubble radius.

Once a structure is equilibrated, we are left with positions of all bubbles and contact forces acting on them; with this information, we can perform further analysis of the foam and deduce the energy of the system and shape of all bubbles.

3.2 Foam Visualisation

While simulation and modelling of foams is the main objective of most researchers in this sub-field of physics, accurate visualisation of bubbles and entire structures can aid in the proper understanding of the problem at hand; hence, the focus of the project was not solely on the simulation aspect, but also on the visualisations.

The shape of a bubble is entirely described by the Green's function in eq. (5). The challenge is to implement it in software capable of producing mathematically described shapes. Python is an extremely versatile and powerful language; it fits perfectly for the creation of the simulation software, but, unfortunately, it lacks a convenient module for pleasing-to-the-eye 3D graphics. Thankfully, there exists an open-source 3D computer graphics software called Blender, which has Python API enabling communication with the software through Python scripts.

Although it is not essential to any particular large-scale task, singularity present in eq. (5) is a side-effect of the Morse-Witten theory, and so, to accurately visualise bubbles in a natural foam it should be removed. There is no one way of capping singularities in the case of a bubble with multiple contacts: The contact areas are not necessarily flat and sometimes hard to define as the indentations caused by singularities may overlap (although, it is unlikely to in the wet limit). It should be obvious by now that the development of a universal method capable of capping any bubble would be significant a challenge.

In Blender, every object can be represented as a mesh, which contains vertices, edges, and faces. A sphere is not perfectly round, but is made of a large number of flat quadrangles (or triangles). To generate a bubble, first, a sphere is created and then given the contact point(s) and corresponding force(s), each vertex is displaced according to eq. (4). It is important then to adjust the centre of the sphere.

The algorithm developed to cap singularities assumes that the contact area is defined by the immediate region around the contact point where the gradient in the axis created by the contact point and centre of mass of a bubble is negative. In pragmatic steps, the algorithm is as follows: vertices are divided into cells with the zeroth cell containing the vertex closest to the contact point and each consecutive cell containing the neighbours of the previous cell whose displacement in the contact-centre axis is at least as large; then going through cells in the reverse order, starting with the second last cell, each vertex is rescaled such that its height is equal to the average of its nearest and next-nearest neighbours from the previous cell. This algorithm was tested on a number of realistic systems and works flawlessly for forces of magnitude lesser than 4 (which is extremely improbable to ever occur in the wet limit).

4 Evaluation

4.1 Equilibration

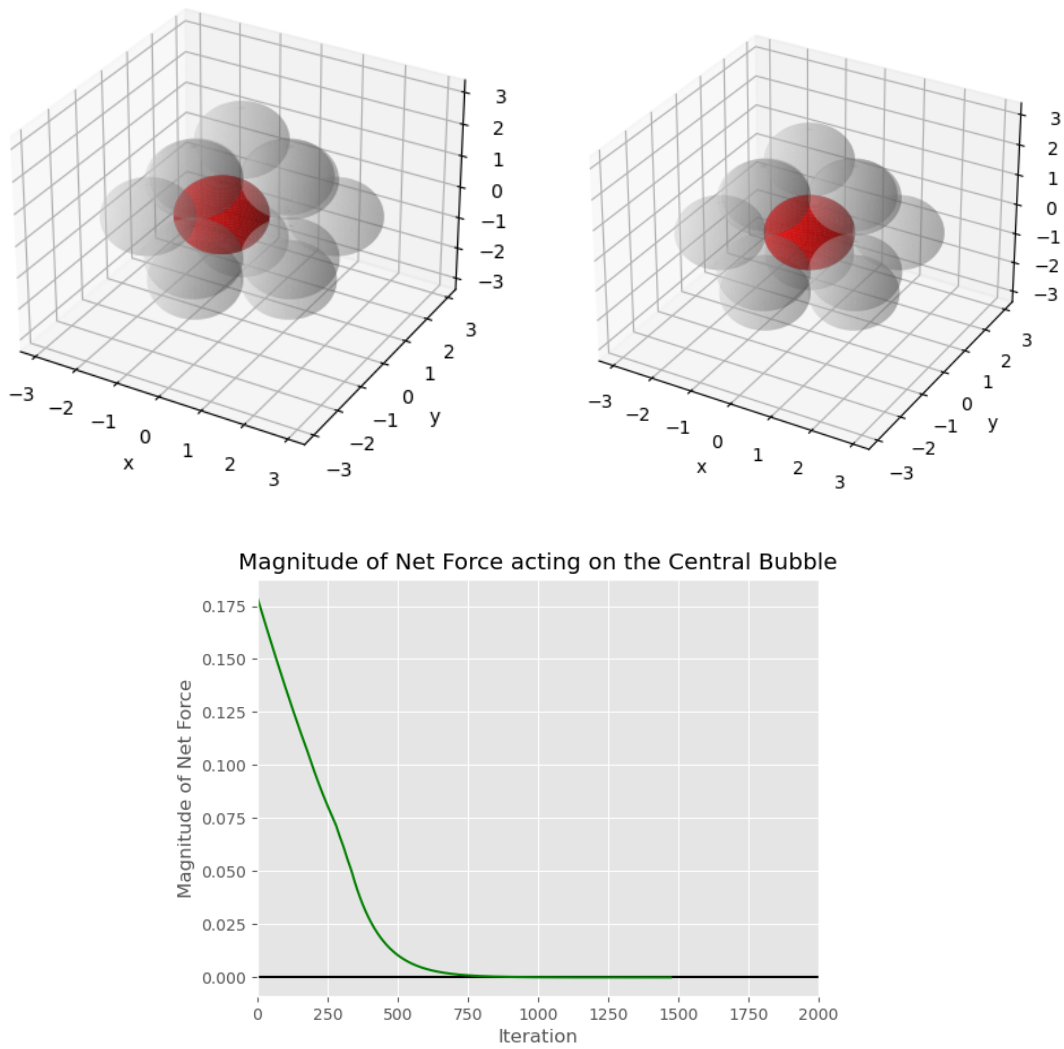


Figure 4.1: FCC structure equilibration using Morse-Witten model and fixed cage constraint (liquid fraction= 0.2). The top left image shows the initial structure, while the top right shows the final, equilibrated structure. As expected from the symmetry, the central bubble was pushed to the origin. The bottom graph shows the magnitude of the net force acting on the central bubble at each step of the process.

Software for equilibration has been developed successfully for both Durian and Morse-Witten models as well as the fixed cage and harmonic potential constraints. The veracity of the program can be easily confirmed by plotting the structure and the magnitude of the net forces acting on the bubbles.

As can be seen in fig. 4.1 and fig. 4.2 the central bubble (coloured red) initially displaced is moved back to the origin as expected from the symmetry of the FCC structure used. Also, the graph of the net force magnitude acting on this bubble confirms that this change indeed reduces the net force acting on the bubble, overall, leading to a state of lower energy.

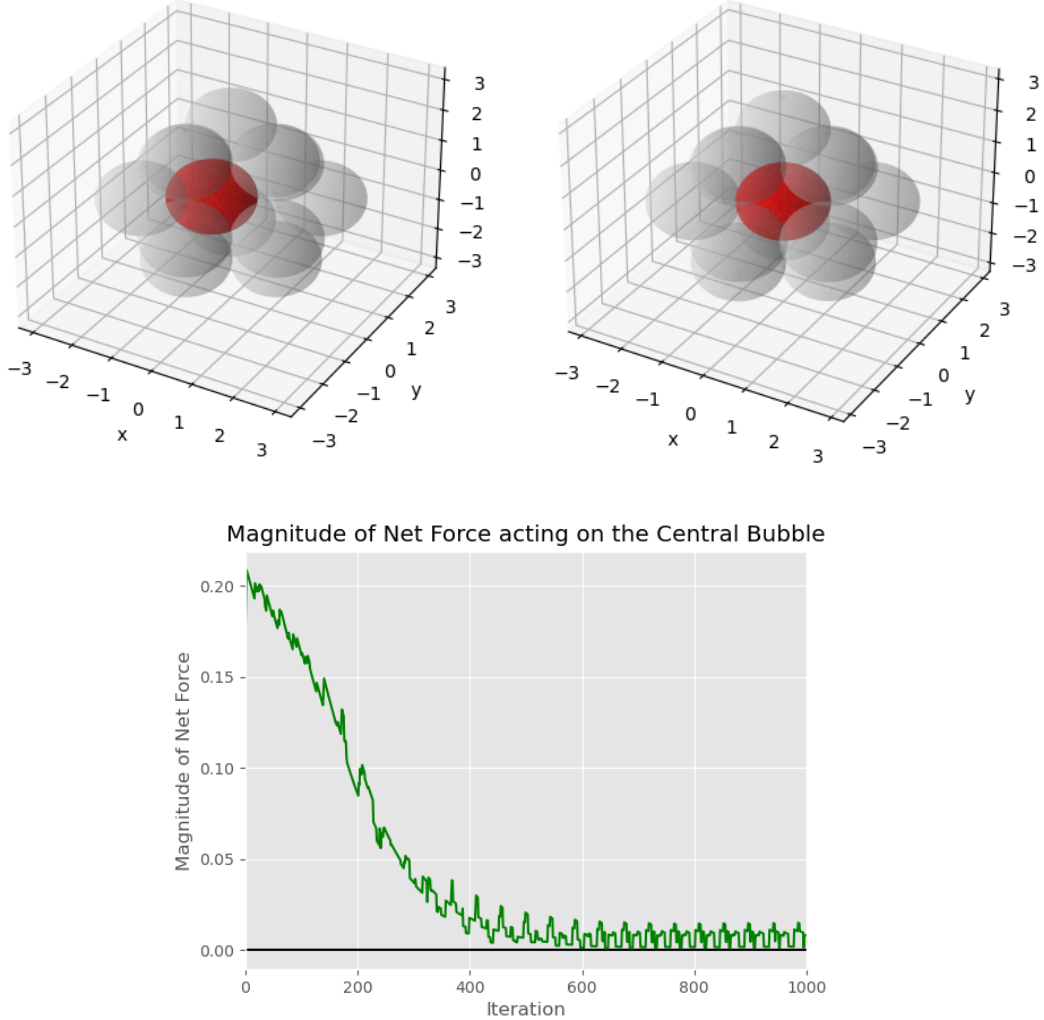


Figure 4.2: FCC structure equilibration using Morse-Witten model and harmonic potential constraint (potential width= 1.9). The top left image shows the initial structure, while the top right shows the final, equilibrated structure. As expected from the symmetry, the central bubble was pushed to the origin. The bottom graph shows the magnitude of the net force acting on the central bubble at each step of the process.

As can be seen in fig. 4.2, the magnitude of the net force acting on the central bubble oscillates in an approximately periodic fashion, especially for the latter half of the equilibration process. This is an interesting feature of the harmonic potential constraint differentiating it from the fixed cage approach. The suggested reason behind this phenomenon is that when the

harmonic potential is used and multiple bubbles are moved by a finite amount at each step, ‘overshooting’ is much more profound, and the force dumping term (i.e., the proportionality constant between the net force and distance moved) needs to be much smaller to reduce bubble oscillations compared to the fixed cage approach where only one bubble changes position. Indeed, this hypothesis is validated, as running the code for lower values of the dumping term produces a smoother curve, though not as smooth as the fixed cage simulation.

4.2 Energy Calculation for Two-Bubble System

To further validate the simulation software, energy was calculated for different widths of the harmonic potential - r_0 in eq. (8) - after equilibration of a structure. Energy contributions came from the potential and from the overlaps/contacts between bubbles, which we call excess energy. Excess energy is the amount by which the energy of a bubble increases after it becomes deformed due to the contact force(s). Mathematically, in the case of the Morse-Witten model, it is $E(\phi) - E_0$, where ϕ is the liquid fraction, and $E_0 = 4\pi\gamma R^2$. Since we vary r_0 instead of ϕ we can also write $E(r_0) - E_0$. In the case of the Durian model, we have $E_0 = 0$, however.

Excess energy for the Morse-Witten model was derived in [12, 19] and is given by

$$E_{\text{MW}} = \frac{1}{8\pi} \sum_i^N f_i^2 \left(\ln \frac{8\pi}{f_i} - \frac{4}{3} \right) + \frac{1}{2} \sum_{i,j \neq i}^N G(\theta_{ij}) f_i f_j. \quad (9)$$

For the Durian model, we use the standard equation for a Hookean spring:

$$E_{\text{Durian}} = \frac{1}{2} \sum_i^N \frac{1}{2} k_D \delta_i^2 = -\frac{1}{2} \sum_i^N \frac{1}{2} \frac{1}{k_D} f_i^2, \quad (10)$$

where an extra factor of $\frac{1}{2}$ is added to account for double-counting of overlaps.

Hereunder $R_0 = 1$, $k_p = 1$, and $k_D = \frac{1}{2}$ will be used for convenience, since it does not require any extra normalisation factors - if, for example, $k_D = 1$ would be used it would imply that $\gamma = 2$ as $k_D = \frac{\gamma}{2}$ and appropriate normalisation factors would need to be added.

4.2.1 Durian Model

Defining the coordinate system such that both bubbles are distance r away from the origin, the total energy given by the Durian model is

$$E_{\text{tot}} = 2E_p + 2E_{\text{Durian}} = 2k_p(r - r_0)^2 + \frac{1}{2}k_D\delta^2, \quad (11)$$

where we labelled the potential energy as E_p . Using elementary calculus and noting that $\delta = 2(R_0 - r)$, we find that E_{tot} is minimised for

$$r^* = \frac{k_p\Delta + k_D R}{k_p + k_D}, \quad (12)$$

which gives

$$E_{\text{tot}}(r^*) = \frac{2k_p k_D}{(k_p + k_D)} (R - \Delta)^2 = \frac{2}{3} (1 - \Delta)^2. \quad (13)$$

To simplify the discussion, however, only overlap energy will be considered, and so,

$$E_{\text{Durian}}(r^*) = \frac{4}{9} (1 - \Delta)^2. \quad (14)$$

The analytical solution together with numerical data is shown in fig. 4.3 (left). Both data sets match perfectly, confirming the veracity of the equilibration process and energy calculations using the Durian model.

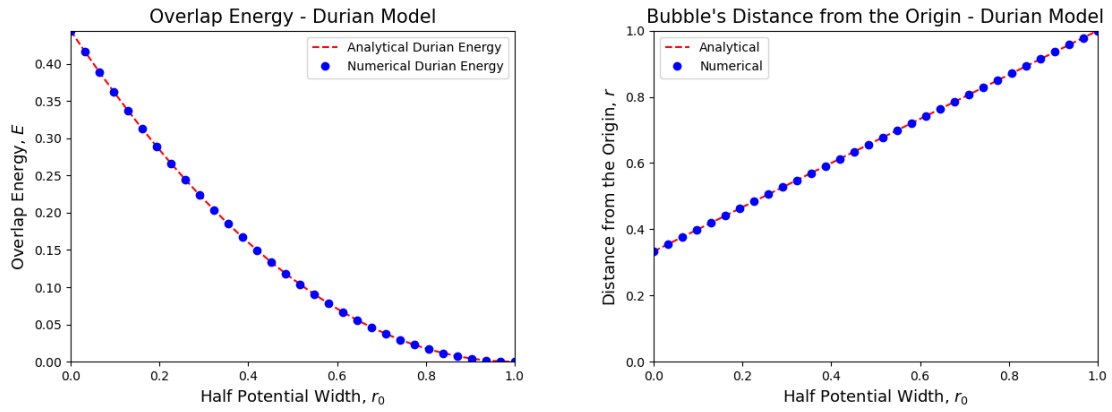


Figure 4.3: Left: Numerical and analytical overlap energy of a two-bubble system as a function of the potential width obtained using the Durian model. Right: Numerical and analytical solution for the equilibrium position of the bubbles in the two-bubble system as a function of the potential width.

We can also plot the numerical equilibrium position of a bubble and compare it to the analytical value presented in eq. (12), which may be a more meaningful comparison when it comes to corroborating the software. The figure is presented in fig. 4.3 (right), and, once again, the numerical data matches the theoretical expectations.

4.2.2 Morse-Witten Model

For the Morse-Witten model, we note that in equilibrium force due to the contact is equal to the potential force, $f_{\text{MW}} = f_p$. To find f_{MW} we take eq. (7) and set $N = 1$, thus, removing the second term from the equation; then, we use Lambertian W function to find the exact solution (see also [1]):

$$f_{\text{MW}} = \frac{4\pi x}{W_{-1}(e^{5/6}x/2)}. \quad (14)$$

Hence, it follows that

$$\frac{4\pi(r^* - 1)}{W_{-1}[e^{5/6}(r^* - 1)/2]} = 2k_p(r^* - r_0), \quad (15)$$

which can be solved to provide a fully analytical solution for the equilibrium position of a bubble, r^* , as a function of the potential width, r_0 . Without providing full calculations, it should be clear that the relation between the potential width and the position of the bubble in equilibrium is non-linear. This is in contradiction to the numerical software, which, at the moment of writing, outputs a linear relationship similar to that expected from the Durian model. The failure of the software to confirm the theory suggests an error in either force calculation or data output methods.

4.3 Foam Visualisation

Thanks to the Blender's convenient API, a Python script was written that generates required shapes and structures within the Blender software using Morse-Witten theory of wet foams and data generated using the main equilibrating software.

A small selection of images presenting the effects of capping and general capabilities of the program developed is shown in the Appendix A1.

Blender has a wide selection of options when it comes to defining not only the colours of materials but also their optical properties. So far, due to time and skill constraints, only simple materials were used in generating images. Note that the type of material used in Blender in no way affects the physical behaviour of a bubble in actual simulation - it is purely for visual effects. In future works, it may be of interest to develop more realistic images with appropriately modified material.

5 Conclusion

To summarise, numerical software for the simulation of three-dimensional foams was successfully developed. Two models of wet foams were implemented: Durian and Morse-Witten; and two types of system constraints were used: fixed cage constraint and harmonic potential constraint. The software equilibrates a given foam structure by iteratively calculating forces acting on bubbles and translating each bubble in the direction of the net force acting on it. This process corresponds to the propagation of the system in the time since soft materials - such as foam - naturally tend towards equilibrium.

The software was then used to calculate the total energy as a function of the potential width for a two-bubble system, as the results for such a simple system can be derived analytically. The numerical values obtained were in close agreement with the theory in the case of the Durian model. For potential widths greater than two, the bubbles were able to spread out enough to lose their contact. As a result, energy vanished for these values. As potential width decreased, bubbles came into contact, and the energy started growing as $c(1 - r_0)^2$, where r_0 is half of the potential width and c a proportionality constant. Energy calculations using the Morse-Witten model provided similar energy relation, however, it was found that the system does not reach the equilibrium state correctly. The distance of a bubble from the origin was found to vary linearly with the potential width, which is correct when dealing with the Durian model, but, for the Morse-Witten theory, we know from analytical calculations that the relationship should not be non-linear. This error suggests a mistake in either the implementation of the net force calculations using the Morse-Witten model or in output methods used.

Additionally, Blender, open-source 3D computer graphics software, was used to produce 3D visualisations of individual Morse-Witten bubbles as well as larger foam systems. This required development of another Python script that would integrate into Blender's Application Programming Interface (API) and generate images using data generated by the main software.

By modifying the form of the potential, it is possible to simulate many various systems. For example, a doctoral student, J. Ryan-Purcell, working under this project supervisor, S. Hutzler, has applied the software to investigation of bubble systems confined in a horizontal liquid-filled cylinder. The main objective of his work is the examination of the mechanical response of the bubble chains as a function of axial compression by varying the length of the cylinder as well as study of bubble buckling.

The software (once the equilibration error is fixed) is now a perfect starting point for the expansion of three-dimensional wet foam simulations to, for example, polydisperse wet foams, or wet foams under gravitational pull. While the simulation of gravity only demands a change of the potential field used, polydispersity would require further-reaching changes to the code

base. Normalisation applied to all values in the above considerations would no longer work with polydisperse bubbles and many equations implemented into the program would need to be re-written.

Although not strictly necessary, optimisation of the software could be beneficial, especially when considering larger systems of more than 50 particles. At the current time, equilibration of an FCC structure - with 13 bubbles - can take up to 4 minutes. The exact amount heavily depends on the potential width used. Smaller width values result in bubbles being more heavily compressed, which not only renders Durian and Morse-Witten models significantly less accurate but also necessitates a larger number of equilibration steps. Assuming that the coordination number of bubbles - that is, the number of contacts each bubble has - does not increase drastically, the execution time should scale linearly with the number of bubbles in the system. A potential factor that would worsen the scalability is the non-local effects of a larger network of bubbles. Since bubbles are translated by a finite amount at each step, they will inevitably oscillate around their equilibrium position as they are soft. To minimise said oscillations smaller step size can be used and the maximum step size can be lowered as well. Nevertheless, oscillation is inescapable, and a larger system may amplify the problem, requiring more and more equilibration steps as the system grows.

Ideally, the software would be improved and expanded so as to provide a basis for research of all kinds of weakly compressed bubble systems or even emulsions as they share many physical properties with foams.

Acknowledgements

I would like to acknowledge the initial work done on the software by and continuous support of doctoral student J. Ryan-Purcell, as well as stimulating weekly discussions with project supervisor S. Hutzler and the aforementioned JRP.

Bibliography

- [1] R. Höhler and D. Weaire, "Can liquid foams and emulsions be modeled as packings of soft elastic particles?", *Advances in Colloid and Interface Science*, vol. 263, p. 19–37, 2019.
- [2] V. D. Lapparent, M. J. Geller, and J. P. Huchra, "A slice of the universe," *The Astrophysical Journal*, vol. 302, 1986.
- [3] A. V. D. Net, W. Drenckhan, D. Weaire, and S. Hutzler, "The crystal structure of bubbles in the wet foam limit," *Soft Matter*, vol. 2, no. 2, p. 129, 2006.
- [4] F. F. Dunne, J. Winkelmann, D. Weaire, and S. Hutzler, "Implementation of morse–witten theory for a polydisperse wet 2d foam simulation," *Philosophical Magazine*, vol. 99, no. 18, p. 2303–2320, 2019.
- [5] D. Frenkel, "Soft condensed matter," *Physica A: Statistical Mechanics and its Applications*, vol. 313, no. 1-2, p. 1–31, 2002.
- [6] M. C. Beard, X. Peng, Z. Hens, and E. A. Weiss, "Introduction to special issue: Colloidal quantum dots," *The Journal of Chemical Physics*, vol. 153, no. 24, p. 240401, 2020.
- [7] A. M. Kraynik, "Foam flows," *Annual Review of Fluid Mechanics*, vol. 20, no. 1, p. 325–357, 1988.
- [8] D. L. Weaire and S. Hutzler, *The physics of foams*. Clarendon Press, 2005.
- [9] W. Drenckhan and S. Hutzler, "Structure and energy of liquid foams," *Advances in Colloid and Interface Science*, vol. 224, p. 1–16, 2015.
- [10] J. R. A. L., *Introduction and overview*, p. 1–2. Oxford University Press, 2003.
- [11] K. A. Brakke, "The surface evolver," *Experimental Mathematics*, vol. 1, no. 2, p. 141–165, 1992.
- [12] D. C. Morse and T. A. Witten, "Droplet elasticity in weakly compressed emulsions," *Europhysics Letters (EPL)*, vol. 22, no. 7, p. 549–555, 1993.
- [13] D. M. Buzzia and M. E. Cates, "Uniaxial elastic modulus of concentrated emulsions," *Langmuir*, vol. 10, p. 4503–4508, Dec 1994.
- [14] L. S. Bragg and J. F. Nye, "Ein dynamisches modell einer kristallstruktur," *Naturwissenschaften*, vol. 34, no. 11, p. 328–336, 1947.

- [15] H. Princen, M. Aronson, and J. Moser, "Highly concentrated emulsions. ii. real systems. the effect of film thickness and contact angle on the volume fraction in creamed emulsions," *Journal of Colloid and Interface Science*, vol. 75, no. 1, p. 246–270, 1980.
- [16] R. Höhler and S. Cohen-Addad, "Many-body interactions in soft jammed materials," *Soft Matter*, vol. 13, no. 7, p. 1371–1383, 2017.
- [17] D. J. Durian, "Foam mechanics at the bubble scale," *Physical Review Letters*, vol. 75, no. 26, p. 4780–4783, 1995.
- [18] S. Cohen-Addad and R. Höhler, "Rheology of foams and highly concentrated emulsions," *Current Opinion in Colloid and Interface Science*, vol. 19, p. 536–548, Dec 2014.
- [19] S. Hutzler, F. F. Dunne, A. M. Kraynik, and D. Weaire, "The energy of fcc and hcp foams," *Soft Matter*, vol. 16, no. 35, p. 8262–8271, 2020.

A1 Appendix

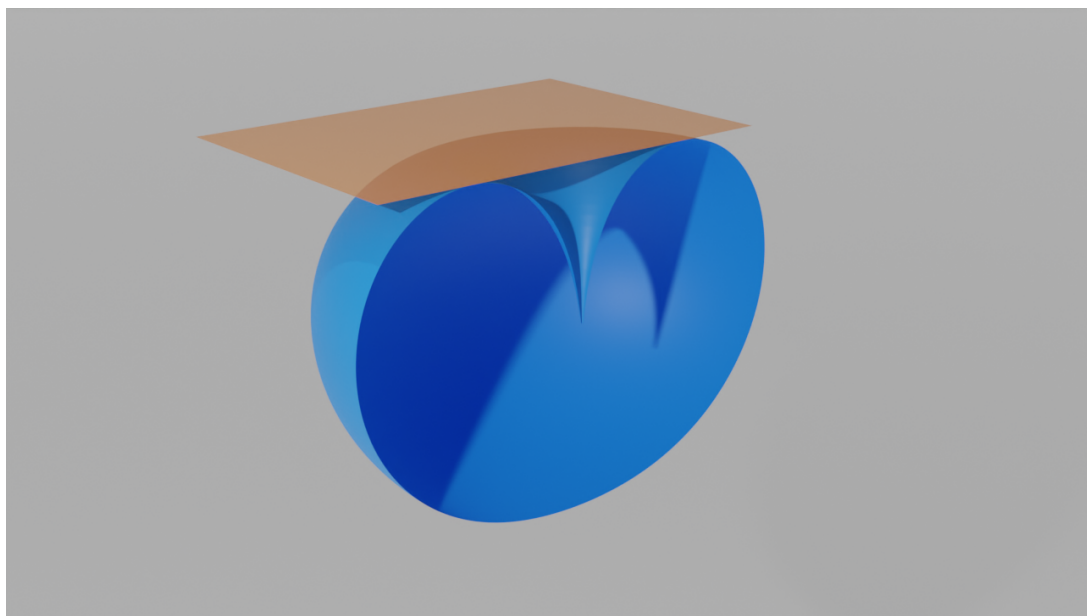


Figure A1.1: A cross-section of a bubble in equilibrium buoyed against a flat wall exerting a vertical point force.

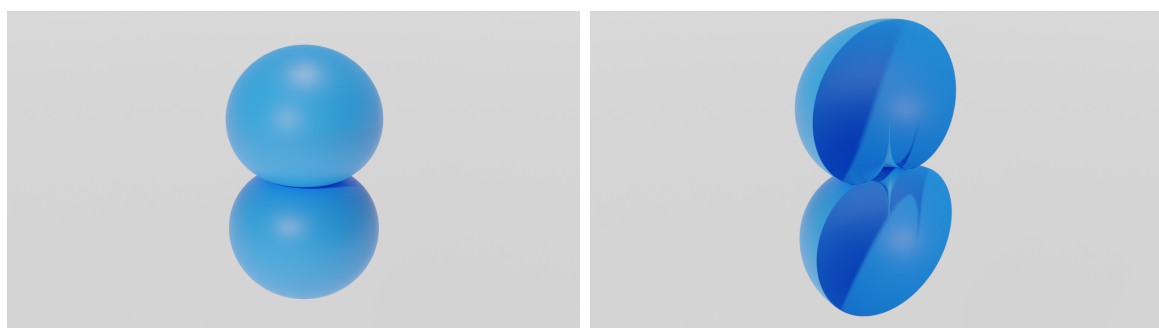


Figure A1.2: Two bubbles pressing against each other with contact force of $f = 2$.

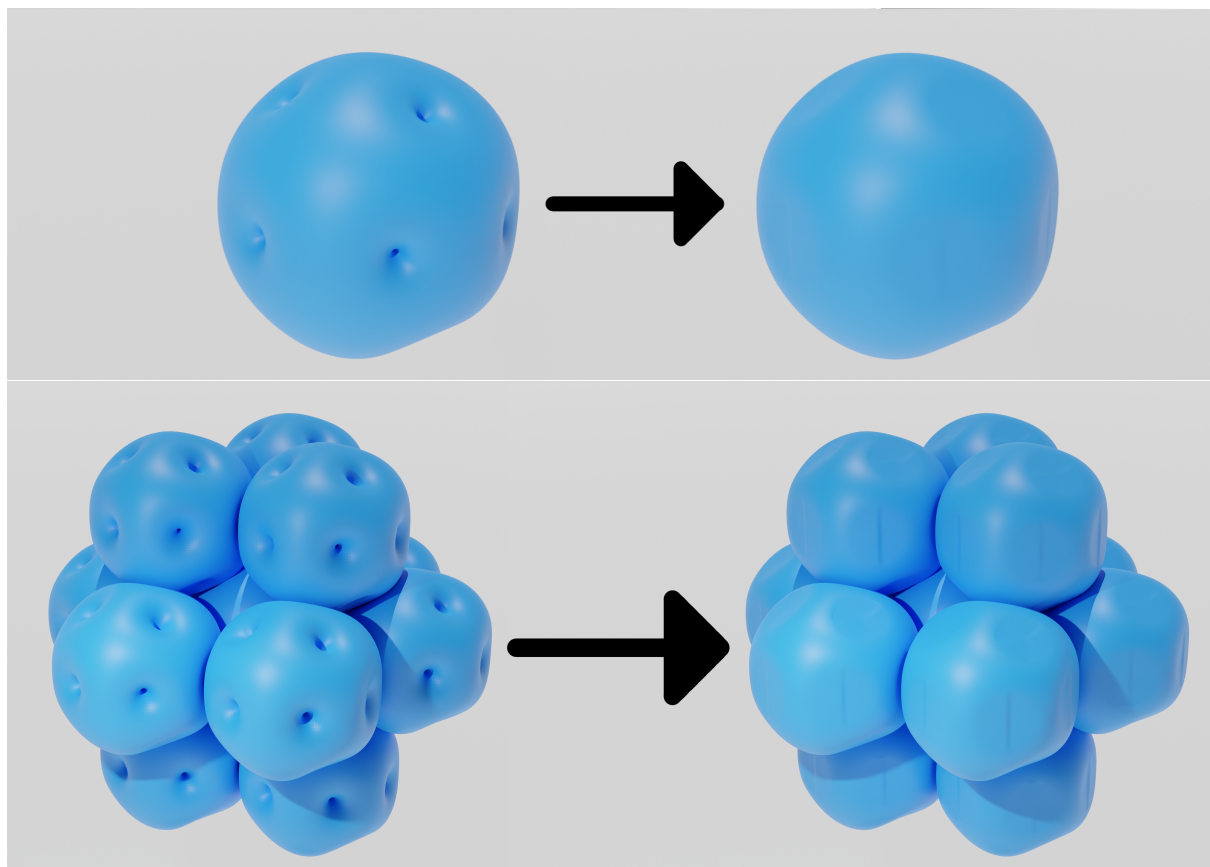


Figure A1.3: Top: A single FCC bubble with and without singularities capped. Bottom: A single FCC cell with and without singularities capped.

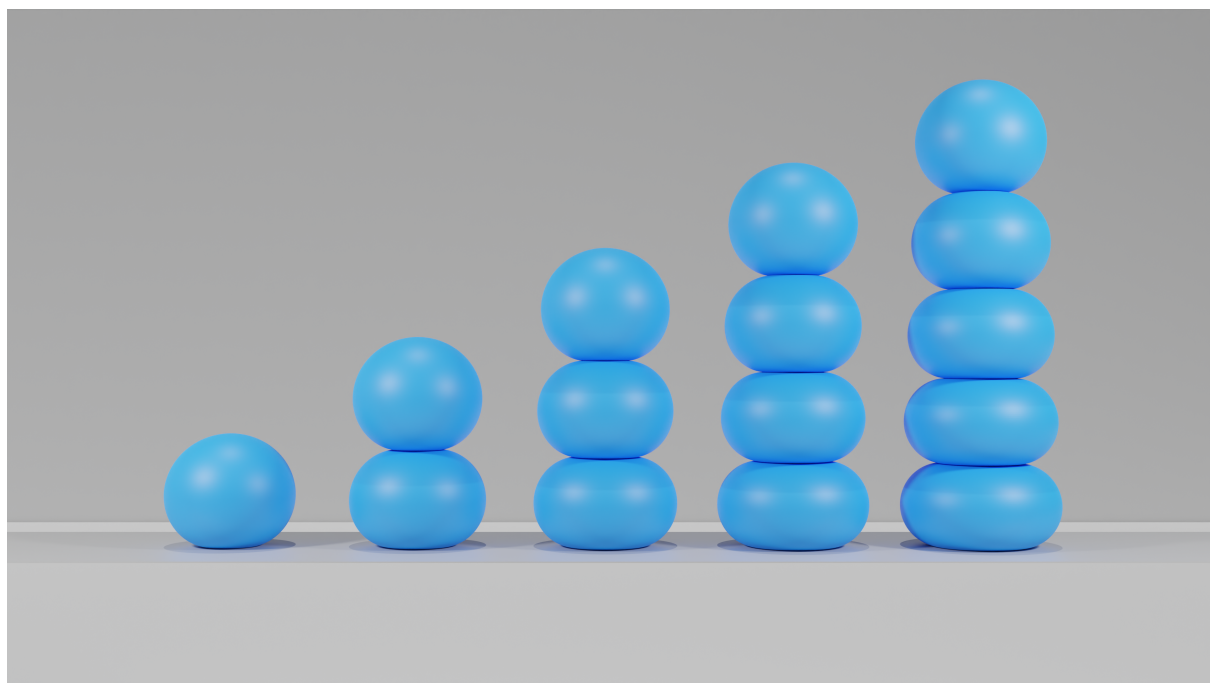


Figure A1.4: Towers of vertically stacked bubbles under gravity.